Extreme Sea Levels on the Mt Maunganui Shoreline (Moturiki Island)

July 1997

NIWA CLIENT REPORT NO 97/32

Project No. VRC70501

Extreme Sea Levels on the Mt Maunganui Shoreline (Moturiki Island)

Derek Goring, Charles Pearson, Sandra Kingsland

prepared for
Environment Bay of Plenty

Information contained within this report should not be used without the prior consent of the client

NIWA
PO Box 8602
Christchurch, New Zealand
Telephone +64-3-348 8987
Facsimile +64-3-348 5547

July 1997

NIWA CLIENT REPORT NO. 97/32

Project No. VRC70501

EXECUTIVE SUMMARY

Twenty three years of continuous sea level data from the Moturiki Island sea level recorder were analysed to estimate annual exceedance probabilities of extreme sea levels using a Revised Joint Probability analysis method (RJP) developed by Tawn and Vassie (1991).

Results indicate that the 1% annual exceedance probability sea level (ie 100 year return period) was estimated to be 1990mm ± 300mm above MSL for the Mt Maunganui shoreline (Moturiki Island).

Storm surge is a stochastic process, therefore we recommend that as additional data become available for Moturiki, the Revised Joint Probability analysis be repeated using the software that has been developed for this project. A copy of this software will be made available to project partners at the end of the project.

TABLE OF CONTENTS

Reviewed by:

Approved for release by:

Project Director

LIST OF FIGURES

LIST OF TABLES

1. INTRODUCTION

This report is one of six resulting from a project commissioned by six councils (Table 1.1) to investigate the risk of sea level inundation caused by the interaction of tides and storm surge. The project was initiated by the event of July 14, 1995 in the Firth of Thames where substantial damage was caused by sea level inundation, yet when the event was analysed it was found that neither the tide nor the storm surge were particularly large. The reason for the high sea levels was that the peak of the storm surge occurred precisely at the time of high tide. Had the peak occurred a few hours earlier or later, there would have been no flooding. Had the peak occurred one high earlier or later, there would have been no flooding. Had the peak occurred one month earlier, there would have been even worse flooding. This event raised the question: what is the probability that moderate storm surge and moderate tides can combine to cause high sea levels like this?

Investigation revealed that the Proudman Oceanographic Laboratory (POL) in Liverpool had recently carried out such a study for the coast of UK (Tawn & Vassie, 1991). Following a visit to POL by Derek Goring, POL supplied the software they used for their UK study. A large part of the study reported here has involved adapting this software to New Zealand conditions and data. Part of this has involved adjusting the program to access sea level data directly from TIDEDA files (TIDEDA is the NIWA hydrological database used by most regional councils). Another aspect of New Zealand data is the generally short record and poor quality of the data. This has meant that instead of carrying out the analysis just once, the program has had to be enhanced so that it can be run every year as more data are acquired. As a supplement to this, the Ministry for Environment has funded the development of the software into a user-friendly package from their Sustainable Management Fund. At the completion of the development, the package will be supplied to the project partners and a course will be given to instruct staff on the use of the package.

Table 1.1 List of project partners and the sea level site of each.

Project Partner	Recorder
Auckland Regional Council	Waitemata
Canterbury Regional Council	Sumner Head
Environment Bay of Plenty	Moturiki Island
Environment Waikato	Tararu
Manawatu-Wanganui Regional Council	Port Taranaki
Southland Regional Council/Invercargill City Council	Waihopai River/Bluff

2. SEA LEVEL VARIATION

2.1 Introduction

Sea level fluctuates in response to a whole spectrum of forcing functions. Each of these functions has a distinctive period or range of periods and the spectrum encompasses periods from minutes up to decades. This gives rise to a range of sea level variation phenomena, as shown in Table 2.1.

Table 2.1 Spectrum of phenomena which affect extreme waves and sea level, with the section in this report which deals with each.

Period Range	Phenomenon	Section
0.25 to 1 hour	Tsunami	-
1 to 6 hours	Seiche	-
6 to 9 hours	Compound- and over-tides	2.7.4
~ 12 hours	Semidiurnal tides	2.7.3
~ 24 hours	Diurnal tides	2.7.2
1.5 to 15 days	Storm surge	2.6
3 months to 1 yr	Seasonal and annual effects	2.5
Interannual	El Niño/Southern Oscillation	2.5
Decades	Secular and eustatic sea level change	-

Some of these phenomena are deterministic and others are stochastic. Tides are deterministic. They are caused by astronomical forces and once they are determined they will always be the same. Storm surge is stochastic. It varies from hour to hour and year to year. Thus, we need to quantify it in statistical terms, for example, as the storm surge which occurs for a percentage of time. In the sections which follow the sea level recorded at Moturiki Island is analysed for the phenomena listed in Table 2.1 and where possible, the magnitude of the phenomenon is identified. For tides this information is likely to be changed only slightly with the acquisition of more data. However, for storm surge, we expect that the statistics will change markedly for every extra year of data that is acquired. In Section 2.8 we present the results of our analysis of Revised Joint Probability (RJP) for the data collected to date. The software which is to be supplied as an output of the MfE contract will enable project partners to update this analysis in future years.

2.2 Data

The twenty three years of continuous sea level data used in this study were obtained from the Moturiki Island sea level recorder, positioned at Lat. 37°63’S Long. 176°18’E (Table 2.2 and Figure 2.1). The recorder has been in operation since 31 December 1973 (Figure 2.2 and Appendix I).

Table 2.2 Location of sea level recorders

Site	Easting	Northing	Latitude	Longitude
Bluff	2151500	5391500	46.59	168.32
Moturiki Island	2791287	6391722	37.63	176.18
Port Taranaki	2599700	6238500	39.05	174.03
Sumner Head	2491700	5737500	43.57	172.77
Tararu	2734300	6449600	37.13	175.52
Waihopai	2151400	5410800	46.42	168.33
Waitemata Harbour	2666647	6483240	36.84	174.75

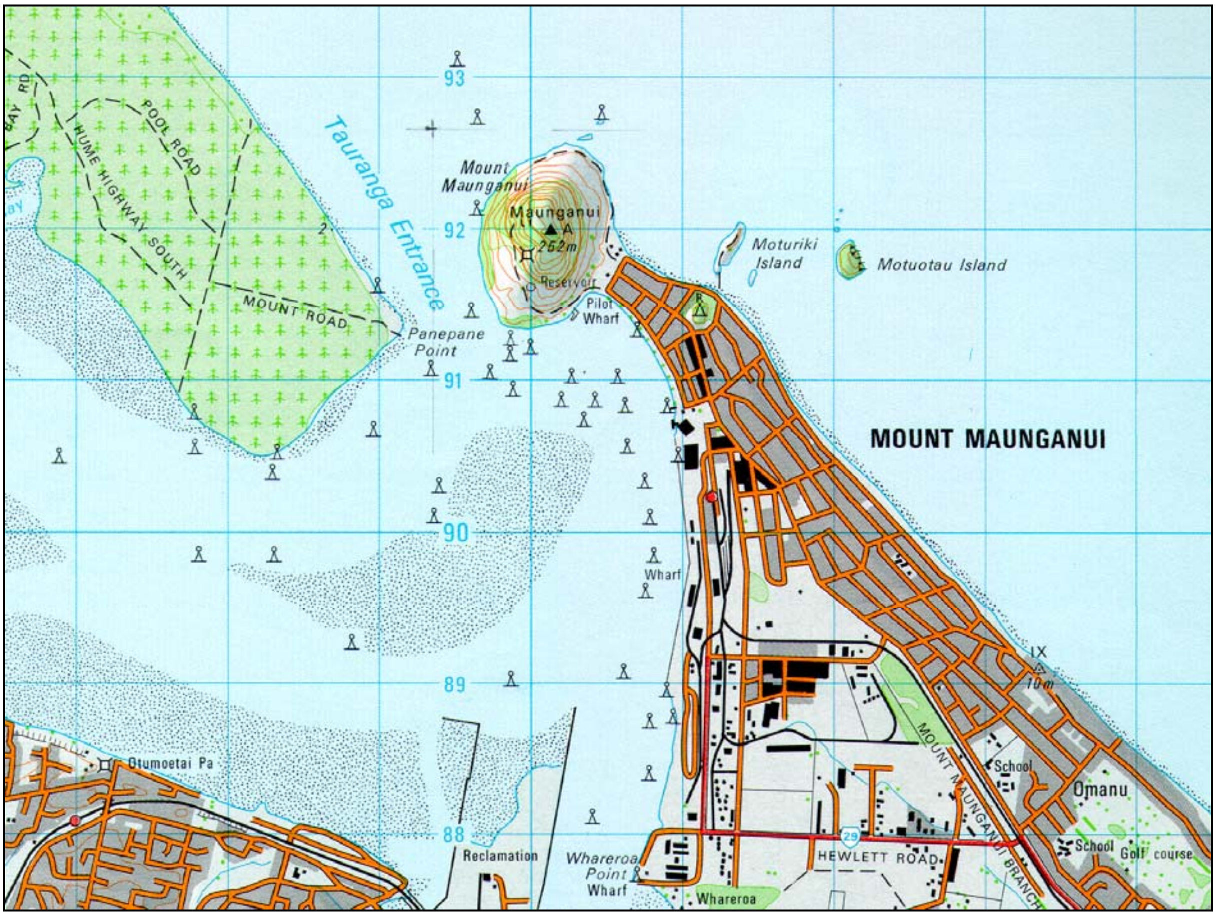

Figure 2.1 Location of the sea level recorder (X). Map reproduced by permission of Land Information NZ: Crown copyright reserved.

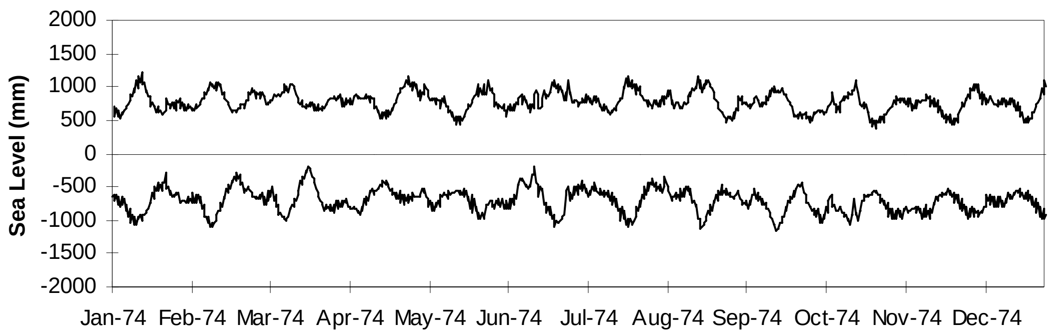

Figure 2.2 Sample envelope of high and low tide for the first calender year of record. The high tide envelope has been calculated by finding the maximum sea level in each tidal period and joining these maxima. The low tide envelope has been calculated in a similar manner.

Gaps in the data, which resulted from equipment failure and maintenance down time, were filled by forecasting the tide and matching the data at either end of the gap. When doing this it was assumed that there was no storm surge for the period of missing data. Of course, this will have some effect on the estimates of probability, with the effect being more serious if the gaps are for long periods and if significant events occur in the gaps. Hence, the importance of having reliable data with few gaps.

2.3 Datum

The datum used in this study was mean sea level (MSL). All estimates of tide and storm surge heights are measured relative to MSL. Mean sea level for Moturiki Island is 1.487m. Zero is defined as -1.487m in Moturiki datum.

2.4 General Analysis

Semidiurnal tides are by far the most important factor in the variation of sea level at Moturiki Island, representing 93% of the variance (or energy) of the signal (Figure 2.3). The remaining 7% is primarily long period effects, with the effect of storm surge, compound tides and diurnal tides being much smaller. Seiche is unimportant for the Mt Maunganui shoreline.

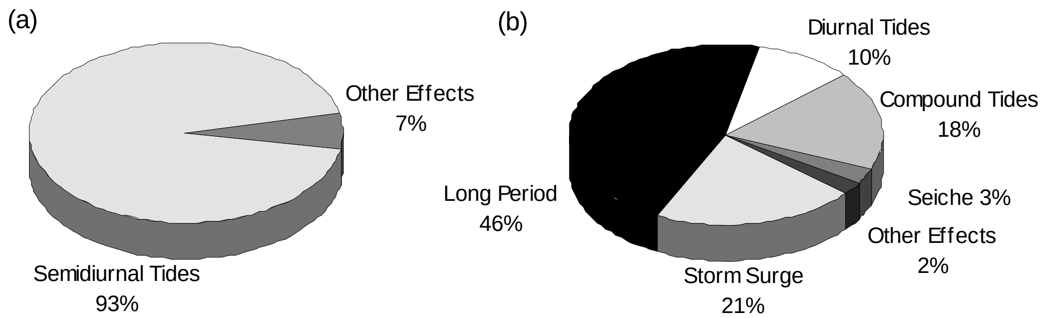

Figure 2.3 How sea level at Moturiki Island is proportioned between causes: (a) overall and (b) for the part excluding the semidiurnal tides.

Of course the data shown in Figure 2.3 represent the overall picture and one reason that tides are by far the most dominant effect is that they occur all the time, whereas storm surge for example occurs only some of the time. Therefore, while it is important to understand and quantify the tide, we must also endeavour to quantify the other effects, even though overall their importance is only 2%. Thus, in the succeeding sections, we address each of these phenomena in turn before combining all of them to estimate the Revised Joint Probability (RJP).

2.5 Long Period Fluctuations

Long period fluctuations have periods greater than 15 days and as indicated in Table 2.1 these include seasonal and annual effects as well as much longer period effects such as El Niño and long-term sea level change. Recent work by Bell and Goring (submitted) has indicated that the major factor influencing these fluctuations on a seasonal and annual basis is sea surface temperature, but on a longer time scale El Nino/Southern Oscillation also has an effect. More data need to be collected at Moturiki Island before any conclusions can be made about the importance of long period waves in determining maximum sea levels on the Mt Maunganui shoreline. In this study the long period waves have been treated as long period tides (Section 2.7.1).

2.6 Storm Surge

In the spectrum of sea level variation (Table 2.1), storm surge lies in the band between 1.5 and 15 days, corresponding to the "weather band". We obtain estimates of storm surge from sea level record by numerically filtering the data to remove the effects of (i) tides and seiche (low pass filtering) and (ii) long period waves (high pass filtering). The overall procedure is termed band pass filtering. The details of the filtering algorithm are described in Goring and Bell (1996). Briefly, it is a boxcar filter with ends tapered using tanh functions. The cutoff frequencies are 1 and 10 °/h (corresponding to 360 and 36 hours respectively) and the tapers have a width of 10 h/°. Filtering is done in the frequency domain. The filtered data are decimated to produce output at 6 h intervals. Figure 2.4 shows the results of band pass filtering the Moturiki Island record, being the record with tides, seiche and long period fluctuations removed.

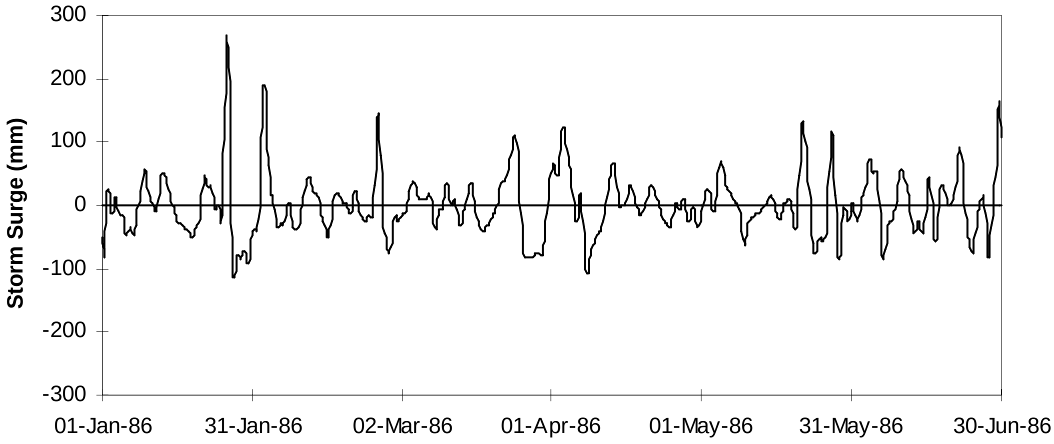

Figure 2.4 Six month period of storm surge at Moturiki Island

2.7 Tides

The tide is caused by the gravitational attraction of the Moon and Sun on the Earth's waters. There are about 600 components in the tide. These are called the tidal constituents and sometimes each constituent is referred to as a tide. Each constituent or tide has a unique frequency governed by astronomical parameters such as the rotation of the Earth and the orbit of the Moon. At any particular place on the Earth's surface, each constituent has a unique amplitude (the height of the tide above and below mean sea level) and a unique phase (its time of occurrence relative to a time datum, usually 0 hours on Jan 1 1900 at Greenwich). Thus, the tide can be represented as a harmonic series:

$$y = \sum_{i=1}^{N} a_i \cos(\omega_i t - \varphi_i) \qquad (1)$$

where y is the observed height above mean sea level and a_i is the amplitude ω_i is the frequency and φ_i is the phase of the i-th constituent. N is the number of constituents in the tide. To identify the tide at a particular location, Equation (1) is used as a model and the amplitudes and phases are fitted numerically to the observed sea level record using some criterion such as least squares. This is called tidal analysis.

The results of the tidal analysis of the Moturiki Island record are presented Table 2.3. The second column of the table contains the name of the constituent in terms of its Darwin symbol (after G H

Darwin, an uncle of Charles Darwin). The symbol often refers to the source of the constituent, thus M stands for Moon and S stands for Sun, but other symbols are more obscure, such as N which represents the ellipticity of Moon's orbit. The subscript denotes the number of times the tide occurs per day. Thus, for example, M_2 is the lunar semidiurnal tide (the twice-a-day tide caused by the Moon's gravitational attraction). The long period tides are different, namely: *a* is annual, *sa* is semiannual, *m* is month and *f* is fortnight.

The third column in Table 2.3 represents the frequency of the constituent in degrees per hour. The table is ordered on increasing frequency and it has been split into sections according to the groups of frequencies. For each group except the long period group, the constituents are bunched around a characteristic frequency which is a multiple of 15 °/h. Some of the constituents have frequencies which are very close together (e.g., S_2 and R_2 where $\Delta f = 0.0410$ °/h). In order to distinguish numerically between one constituent and another, the separation must be: $\Delta f > 360 / T$, where T is the length of record in hours. Thus, for example, to separate S_2 and R_2 we need a record of length $T > 360 / \Delta f = 360 / 0.0410 = 8780h = 366 days.$ Hence, the number of constituents which can be identified depends on the length of record available for analysis. To identify all 600 constituents we need 18.6 years of continuous data. However, most of the 600 constituents are very small and can be neglected. Hence, for this analysis we have split the record into 12 month periods and identified just 60 constituents for each year, then averaged each constituent over the 23 years of data.

The fourth and fifth columns of Table 2.3 give the fitted amplitude and phase respectively of each of the constituents. Constituents with amplitudes less than 5 mm are usually neglected as being insignificant, but have been included here to show that they have been considered.

In the sub-sections which follow, we consider each of the tidal groups in turn and comment on the importance or otherwise of these groups to the maximum tidal height.

Table 2.3 Results of tidal analysis on 23 years of Moturiki Island data. The results represent the average tides from 23 annual analyses.

Tide Type	Constituents	Frequency	Amplitude	Phase (deg)
Long Period	S_a	0.0411	40	36.6

	S_{sa}	0.0821	4	203.7
	M_m	0.5444	2	178.5
	MS_f	1.0159	2	162.4
	M_f	1.0980	8	245.4
Diurnal	$2Q_1$	12.8543	1	5.3
	σ_1	12.9271	1	352.2
	Q_1	13.3987	1	55.4
	ρ_1	13.4715	0	332.3
	O_1	13.9430	12	132.8
	MP_1	14.0252	0	32.8
	M_1	14.4921	0	356.5
	χ_1	14.5695	0	206.0
	π_1	14.9179	2	182.5
	P_1	14.9589	17	169.9
	S_1	15.0000	6	47.1
	K_1	15.0411	54	174.3
	ψ_1	15.0821	1	29.4
	φ_1	15.1232	1	35.0
	θ_1	15.5126	1	207.5
	J_1	15.5854	4	200.0
	SO_1	16.0570	1	238.7
	OO_1	16.1391	2	232.7
Semidiurnal	OQ_2	27.3417	1	140.5
	MNS_2	27.4238	5	109.3
	$2N_2$	27.8954	20	126.1
	μ_2	27.9682	22	128.5
	N_2	28.4397	154	156.1
	υ_2	28.5126	29	156.5
	OP_2	28.9020	4	158.1
	M_2	28.9841	725	191.2
	MKS_2	29.0662	2	291.6
	λ_2	29.4556	4	232.6
	L_2	29.5285	16	235.4
	T_2	29.9589	10	298.8
	S_2	30.0000	94	268.2
	R_2	30.0411	3	135.9
	K_2	30.0821	21	260.9
	MSN_2	30.5444	1	145.1
	KJ_2	30.6265	1	25.0
	$2SM_2$	31.0159	1	144.7
Compound and Overtides	MO_3	42.9271	1	14.3
	M_3	43.4762	5	358.3
	SO_3	43.9430	0	106.0
	MK_3	44.0252	0	81.7
	SK_3	45.0411	4	309.4
	MN_4	57.4238	1	124.8
	M_4	57.9682	0	222.3
	SN_4	58.4397	0	304.8
	MS_4	58.9841	1	66.0
	MK_4	59.0662	0	76.7
	S_4	60.0000	1	195.4
	SK_4	60.0821	1	115.6
	$2MN_6$	86.4079	2	276.0
	M_6	86.9523	3	321.4
	MSN_6	87.4238	0	344.7
	$2MS_6$	87.9682	1	94.7
	$2MK_6$	88.0503	0	90.3
	$2SM_6$	88.9841	0	251.6
	MSK_6	89.0662	0	238.8

2.7.1 Long Period Tides

Figure 2.5 compares the Fourier transform of the Moturiki Island data with the calculated amplitudes of the long period constituents. The dashed line in the figure represents how the measured data are distributed with frequency and the solid line represents what proportion of that is attributable to long period tide. The figure shows that the long period tides, unlike the short period tides to be described in subsequent sections, hardly stand out from the other parts of the sea level signal. On this basis, the amplitudes and phases of the long period tides listed in Table 2.3 must be considered as only a rough estimate of the long period tides. Indeed, Bell and Goring (submitted) in their analysis of 23 years of data from Moturiki Island found that annual and semi-annual constituents are more likely to comprise contributions from variations in sea surface temperature than astronomical forces. In this study we have treated these constituents as tides, but we recognise that as more data become available from Moturiki Island, the long period waves and tides need to be revisited.

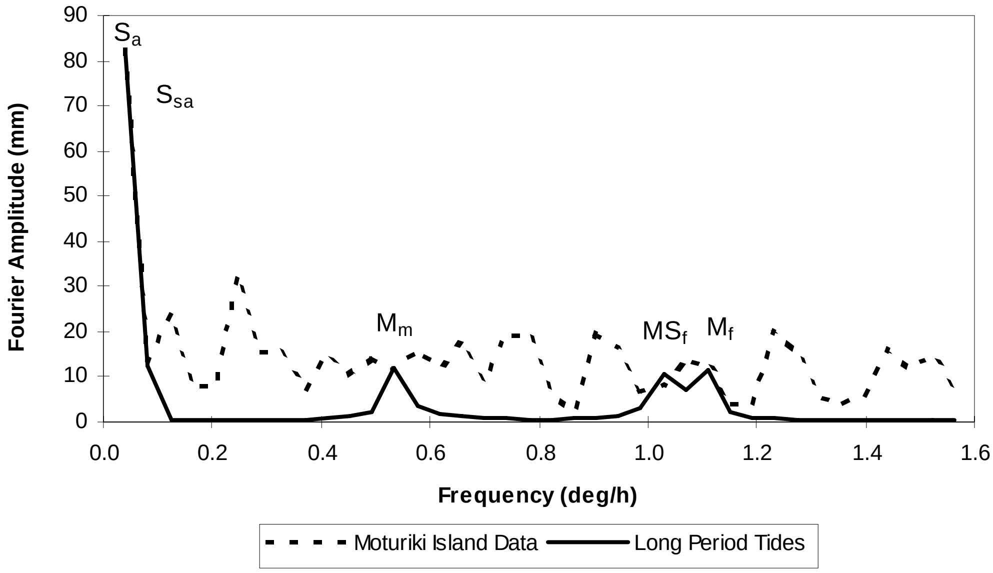

Figure 2.5 Comparison of spectra from Moturiki Island data and the modelled long period tides.

2.7.2 Diurnal Tides

Only four of the diurnal tides are considered significant:

Q_1 - a lunar parallax diurnal tide
O_1 - a lunar declinational diurnal tide
P_1 - a solar declinational diurnal tide
K_1 - a lunar-solar declinational diurnal tide

The S_1 constituent has an amplitude of 5 mm but is more likely to be the result of daily meteorological or temperature effects than to the Sun's gravitational attraction. Nevertheless, it is included as a tide because we have no other way of accounting for these effects. Figure 2.6, comparing the spectra of actual data with fitted tides, shows that in contrast to the long period tides which barely rise above the background data, the diurnal tides appear as distinct spikes in the data.

The diurnal tides are the cause of the sawtooth fluctuations in the tidal envelope (Figure 2.2), causing alternate high tides to differ in amplitude by as much as 150 mm.

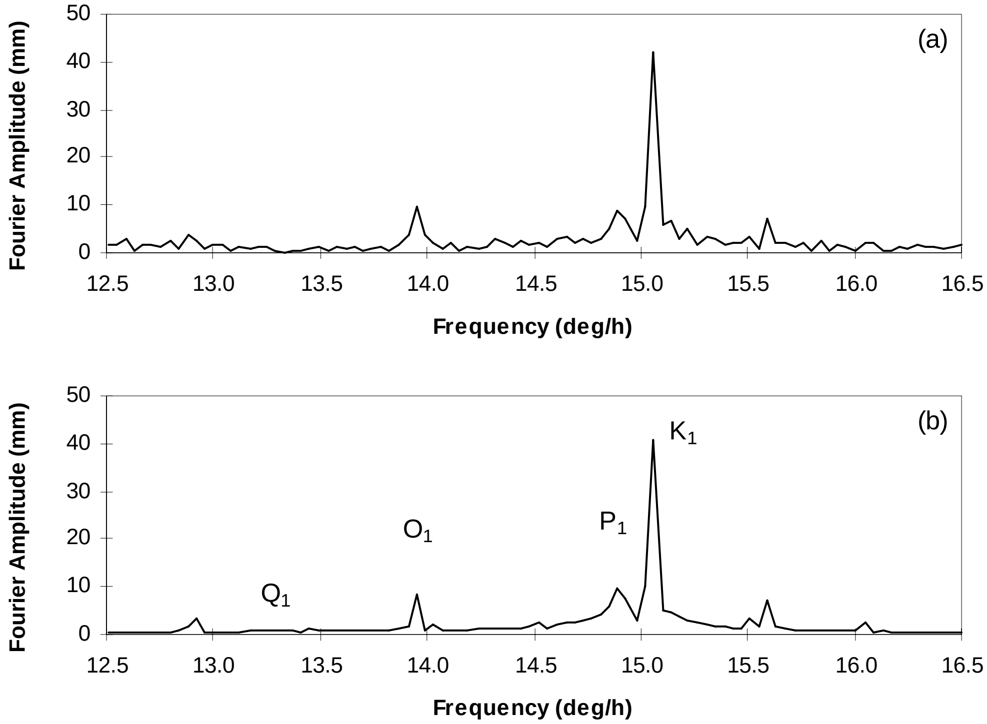

Figure 2.6 Fourier amplitude spectra for the diurnal band of (a) Moturiki Island data and (b) the modelled tide.

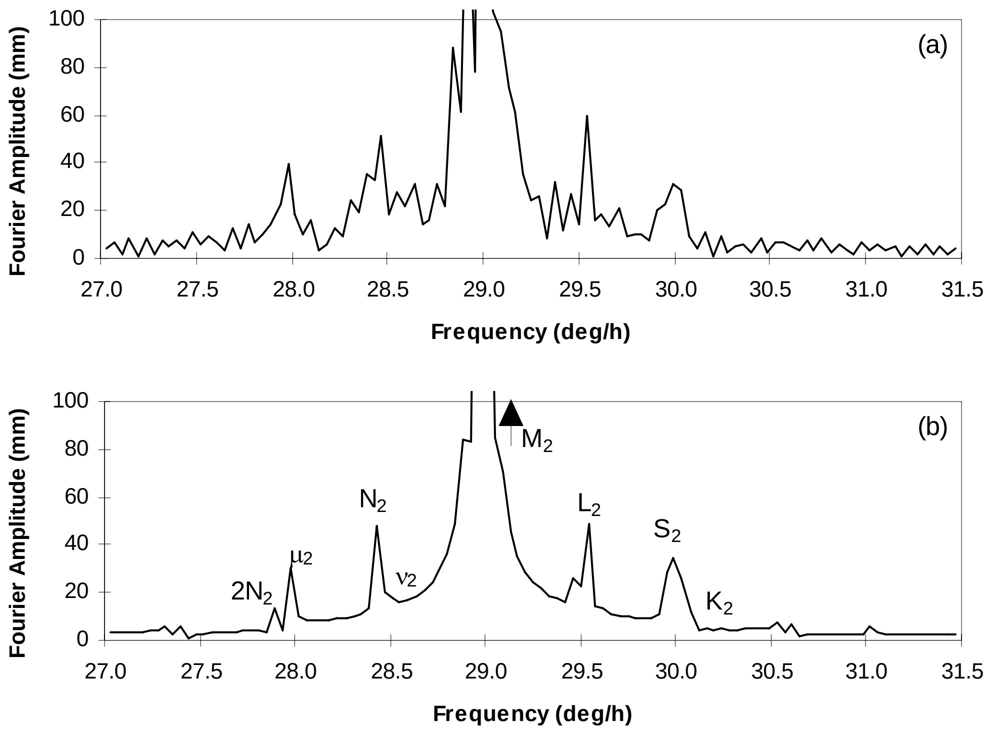

Figure 2.7 Fourier amplitude spectra for the twice daily band (semidiurnal) of (a) Moturiki Island data and (b) the modelled tide. The N_2 and M_2 tides have been truncated so that the other smaller tides can be seen.

2.7.3 Semidiurnal Tides

The semidiurnal frequency band is by far the most important of all. In fact, for Moturiki Island this band represents 95% of the energy in the tide and 93% of the energy in the total signal. Figure 2.7 shows that for the semidiurnal band the spikes in the data do occur at the frequencies expected.

The three major semidiurnal constituents are:
M_2 - the lunar semidiurnal tide;
N_2 - the elliptic semidiurnal tide;
S_2 - the solar semidiurnal tide.

Every 221 days these three constituents combine to produce perigean spring tides. These occur when the Moon is in its perigee (i.e., it is closest to the Earth in its elliptical orbit) and its phase is either Full or New (see Table 2.4). These are the times when a small storm surge could cause major inundation if it were to coincide with high tide.

Table 2.4 List of dates between 1997 and 2005 when Moon's perigee coincides with a Full or New Moon. The largest tides will occur a day or two after these dates. Large tides will also occur 28 days before and after these dates when Moon's perigee almost coincides with Full or New Moon.

February 8, 1997
September 9, 1997
March 28,1998
November 4, 1998
May 16, 1999
December 23, 1999
July 2, 2000
February 8, 2001
September 17, 2001
March 29, 2002
October 6, 2002
April 17, 2003
November 24, 2003
June 3, 2004
January 10, 2005

2.7.4 Compound and Overtides

As the primary tides propagate into shallow water, the frictional effect of the bottom causes nonlinear effects which result in the generation of compound and overtides. Compound tides occur when different tides interact (for example, when the M_2 tide interacts with the N_2 tide, the MN_4 compound tide results). Overtides result from nonlinear effects on the same tide (for example, the M_2 tide generates M_4 and M_6 overtides).

For Moturiki Island, Table 2.3 shows that the compound and overtides are generally less than 4 mm in magnitude.

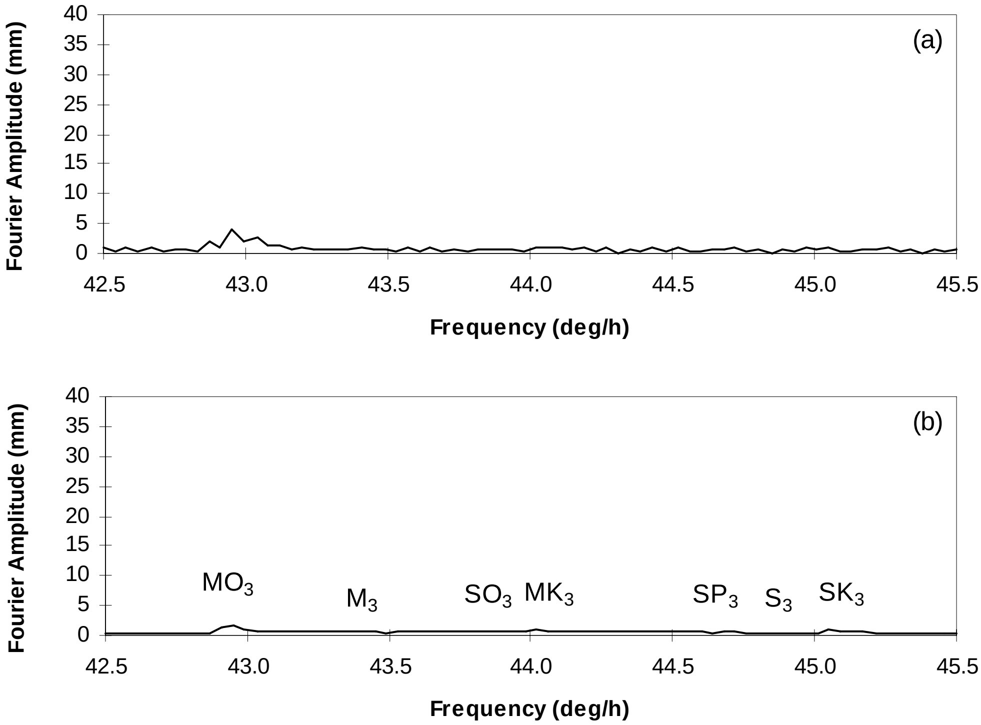

Figure 2.8 Fourier amplitude spectra for one third of the diurnal band (terdiurnal) of(a) Moturiki Island data and (b) the modelled tide.

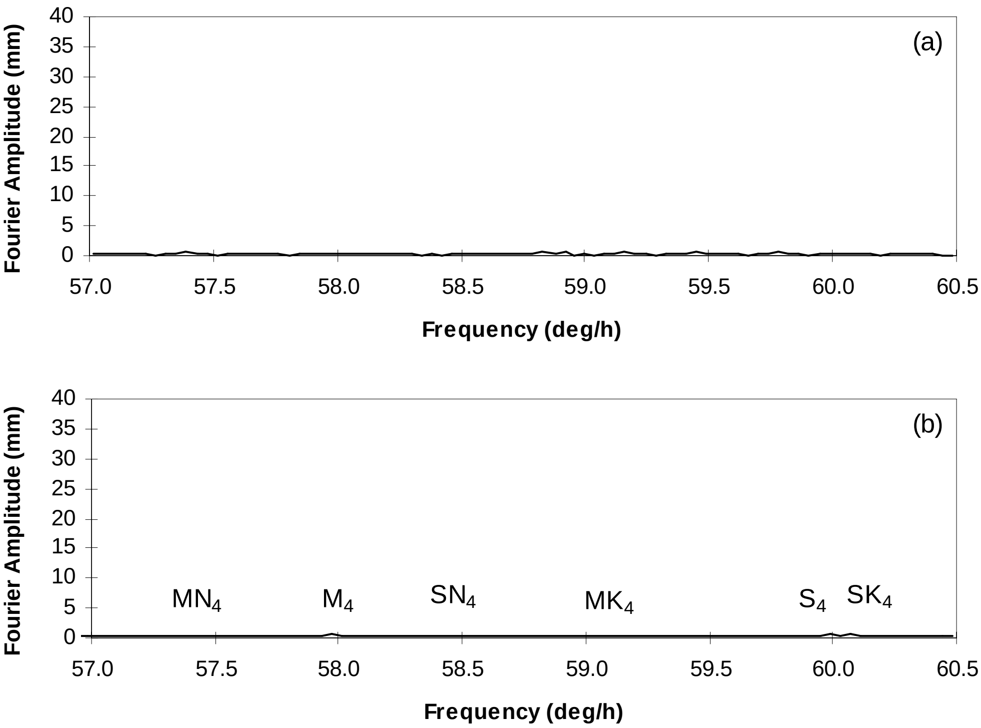

Figure 2.9 Fourier amplitude spectra for one fourth of the diurnal band (quarterdiurnal) of (a) Moturiki Island data and (b) the modelled tide.

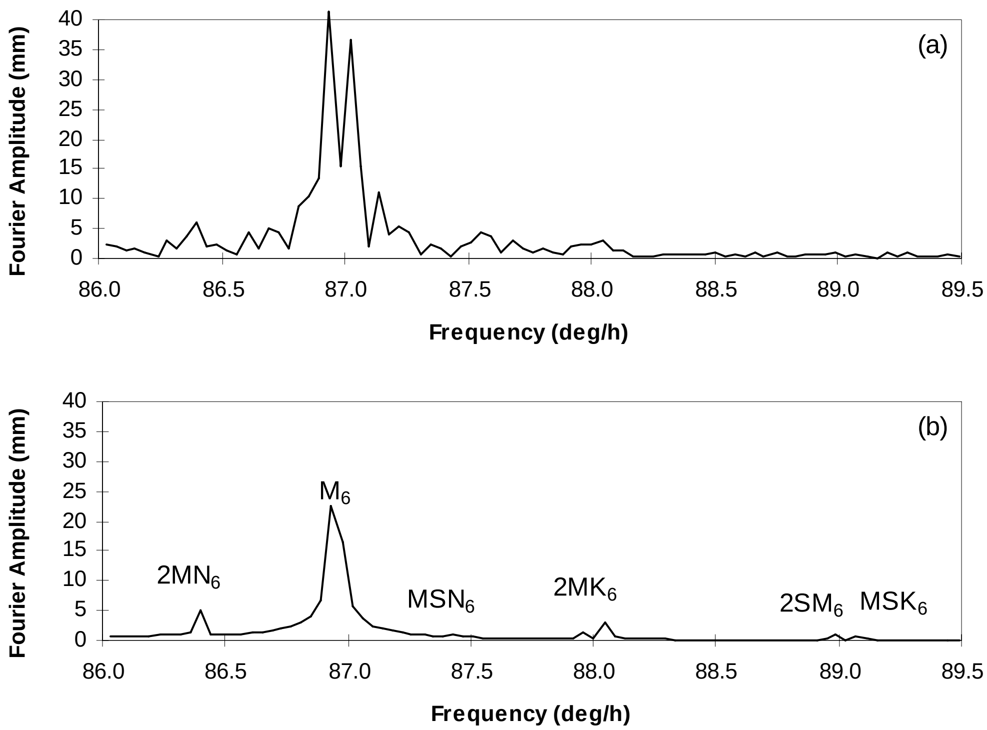

Figure 2.10 Fourier amplitude spectra for one sixth of the diurnal band (sextodiurnal) of (a) Moturiki Island data and (b) the modelled tide.

2.7.5 Combined Tides

To complete this section on tides, we present the results of using the constituents in Table 2.3 to forecast 18.6 years of high tides at Moturiki Island (Figure 2.11). 18.6 years is an important duration because it represents the period over which all the constituents combine in a unique way.

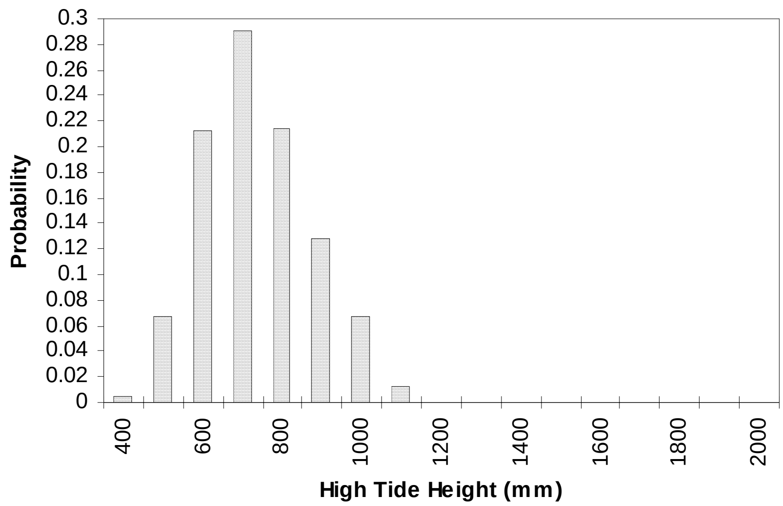

Figure 2.11 Probability distribution for high tide heights at Moturiki Island from 18.6 years of tides forecast using the tidal constituents in Table 2.3.

An important parameter which arises from the data used to prepare Figure 2.11 is the maximum high tide height of 1121 mm above MSL. This is a true maximum in the sense that it is the upper limit of the tide. It will occur once every 18.6 years. Another maximum which can be obtained from Table 2.3 is the sum of the amplitudes of all the constituents, which comes to 1296 mm above MSL. This is the tide height which would occur if the constituents all lined up in phase. However, it can never occur in practice and the maximum from Figure 2.11 is the correct one to use.

2.8 Revised Joint Probability

The method used in this study to estimate annual exceedance probabilities of extreme sea levels is the "Revised Joint Probability Method" (RJPM, Tawn and Vassie 1991), which improved upon the original joint probability method of Pugh and Vassie (1980). As with the joint probability method, the RJPM uses both the sea level (including tides) and storm surge time series data. This provides better estimates than the conventional annual maxima approach applied to the sea level data only, especially when the sea level record is short.

A full description of the RJP method is provided with the documentation and help files for the Extlev computer program, which will be made available to project partners at the end of the project.

Features and options of the RJP method are:
1. it allows for interaction between sea level and surge data (assumed to be the case for this site);
2. it allows for clustering of exceedances;
3. incorporation of linear and quadratic trends in the time series (not used in this study);
4. selection of the r-largest annual maxima (r = 10 for this site);
5. use of either the Generalised Extreme Value (GEV) distribution or the Gumbel distribution, which is a special case of the GEV distribution.

Parameters and statistical tests associated with these options are examined to produce the best RJPM estimates of annual exceedance probabilities of extreme sea levels. These are presented in Table 2.5 and Figure 2.12 for Moturiki Island where the GEV distribution was better for this site.

Table 2.5 Best RJP method estimates of annual exceedance probabilities of extreme sea levels for Moturiki Island with standard errors.

Exceedance Probability	Extreme Sea Level (mm)	Standard Errors
0.2000	1310	40
0.1000	1420	70
0.0500	1550	110
0.0200	1780	200
0.0100	1990	300
0.0050	2240	420
0.0020	2650	640
0.0010	3030	850
0.0005	3470	1100
0.0002	4170	1530
0.0001	4800	1930

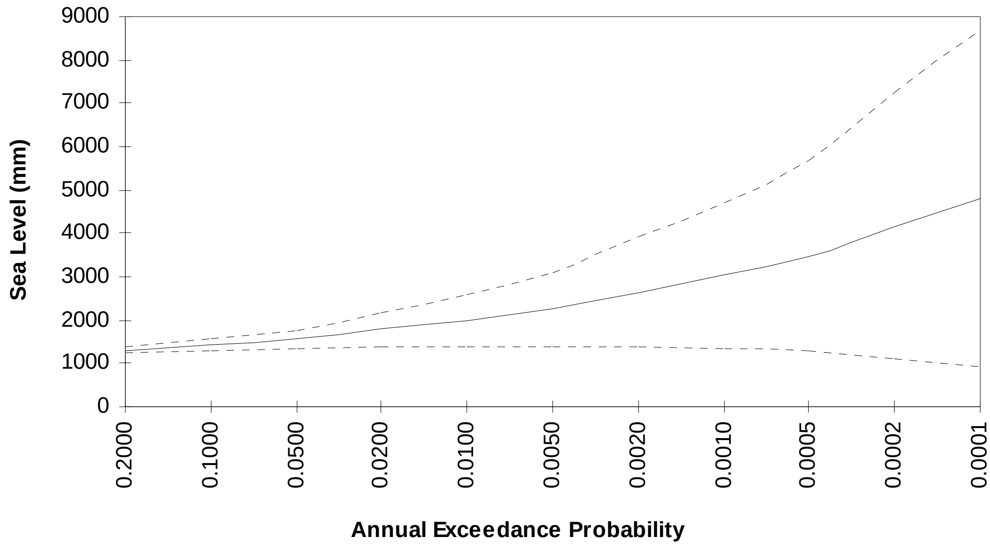

Figure 2.12 Best RJP method estimates of annual exceedance probabilities of extreme sea levels for Moturiki Island with 95% confidence limits (dashed lines).

3. SUMMARY AND CONCLUSIONS

Extreme sea levels on the Mt Maunganui shoreline are caused by the combined tides and storm surge. In this study we have calculated the probability of extreme sea levels using hourly sea level data from Moturiki Island. The data extend from 31 December 1973 to 25 December 1996. Gaps in the data have been filled using tidal forecasts.

The maximum high tide at Moturiki Island is 1121 mm above MSL. Tides of this height will occur every 18.6 years.

Results from the Revised Joint Probability analysis (Section 2.8) show that the 1% annual exceedance probability sea level for Moturiki Island is estimated to be 1990mm (± 300mm) above MSL (ie the estimated 100-year return period sea level).

Extrapolations beyond the 1% annual exceedance probability estimate are provided in Table 2.5 and Figure 2.12. Considering the short record at this site, it is recommended that these extrapolations are used as indicators only.

We expect that the tidal analysis which has been carried out here will be adequate and will not need to be repeated (the tide is deterministic). However, storm surge is a stochastic process, therefore we recommend that as additional data become available for Moturiki Island, the Revised Joint Probability analysis be repeated using the software that has been developed for this project.

REFERENCES

Bell, R. G. & Goring, D. G. 1996: Techniques for analyzing sea level records around New Zealand. *Marine Geodesy*, 19:77-98.

Bell, R. G. & Goring, D. G. (submitted): Seasonal variability of sea level and sea surface temperature on the north-east coast of New Zealand. Submitted to *Estuarine Coastal and Shelf Science*.

Goring, D. G. & Bell, R. G. 1996: Distilling information from patchy tide gauge records: the New Zealand experience. *Marine Geodesy*, 19:63-76.

Pugh, D. T. & Vassie, J. M. 1980 Applications of the joint probability method for extreme sea level computations. Proceedings of the Institute of Civil Engineering 69, 959-975.

Tawn, J. A. & Vassie, J. M. 1991 Recent improvements in the joint probability method for estimating extreme sea levels In Tidal Hydrodynamics (Parker, P. B., ed.). John Wiley & Sons, Inc. pp. 813-828.

APPENDIX I

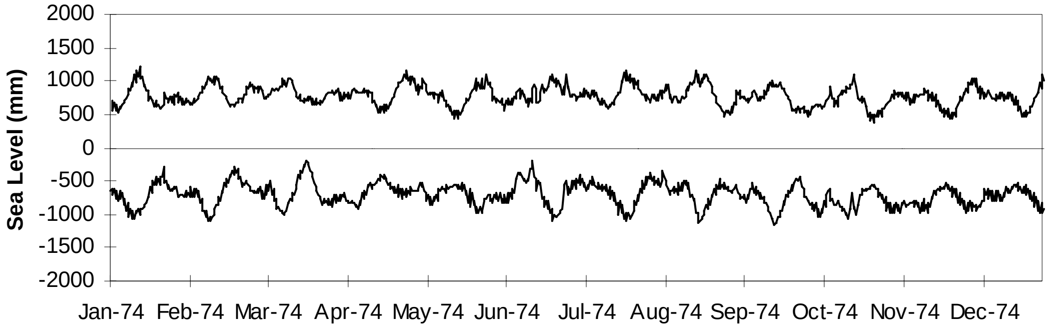
Sea Level (mm)
2000
1500
1000
500
0
-500
-1000
-1500
-2000
Jan-74 Feb-74 Mar-74 Apr-74 May-74 Jun-74 Jul-74 Aug-74 Sep-74 Oct-74 Nov-74 Dec-74

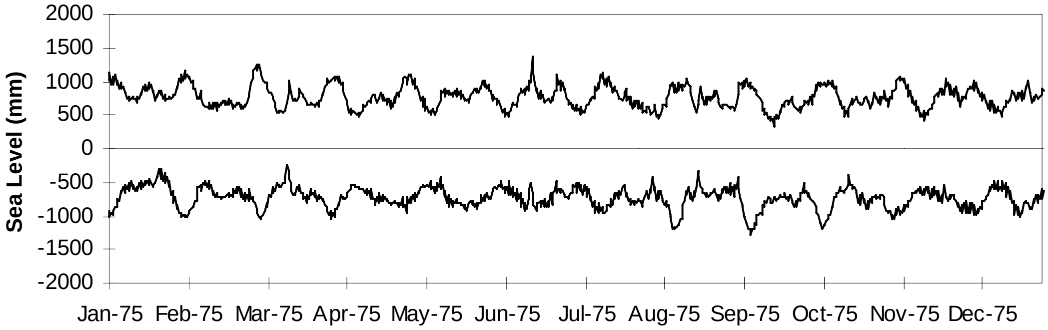
Sea Level (mm)
2000
1500
1000
500
0
-500
-1000
-1500
-2000
Jan-75 Feb-75 Mar-75 Apr-75 May-75 Jun-75 Jul-75 Aug-75 Sep-75 Oct-75 Nov-75 Dec-75

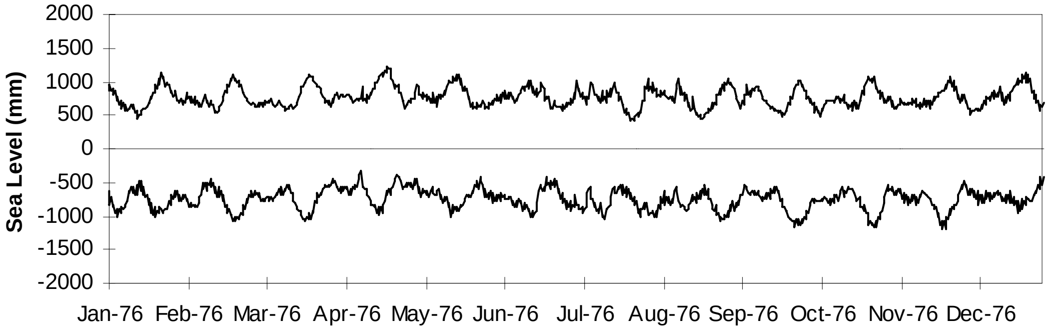
Sea Level (mm)
2000
1500
1000
500
0
-500
-1000
-1500
-2000
Jan-76 Feb-76 Mar-76 Apr-76 May-76 Jun-76 Jul-76 Aug-76 Sep-76 Oct-76 Nov-76 Dec-76

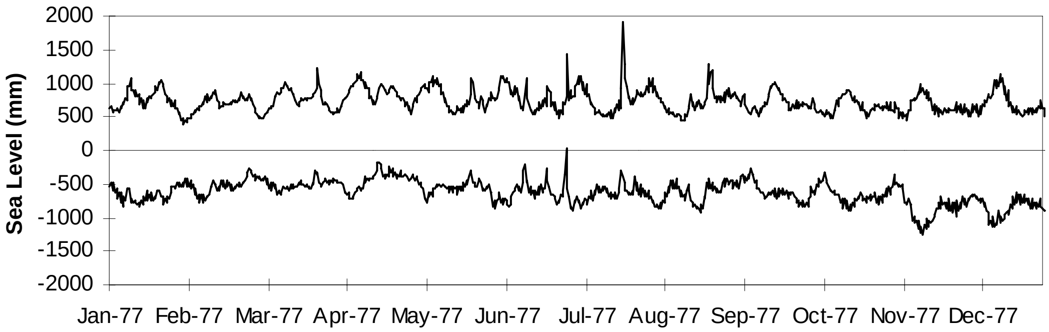
Sea Level (mm)
2000
1500
1000
500
0
-500
-1000
-1500
-2000
Jan-77 Feb-77 Mar-77 Apr-77 May-77 Jun-77 Jul-77 Aug-77 Sep-77 Oct-77 Nov-77 Dec-77

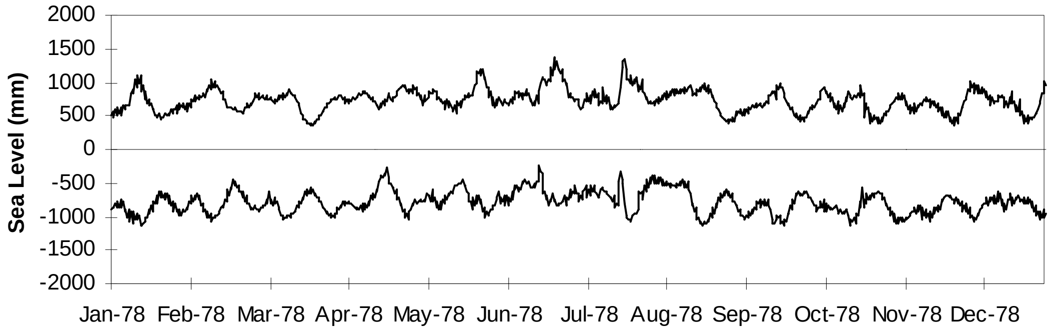
2000
1500
1000
500
0
-500
-1000
-1500
-2000
Sea Level (mm)
Jan-78 Feb-78 Mar-78 Apr-78 May-78 Jun-78 Jul-78 Aug-78 Sep-78 Oct-78 Nov-78 Dec-78

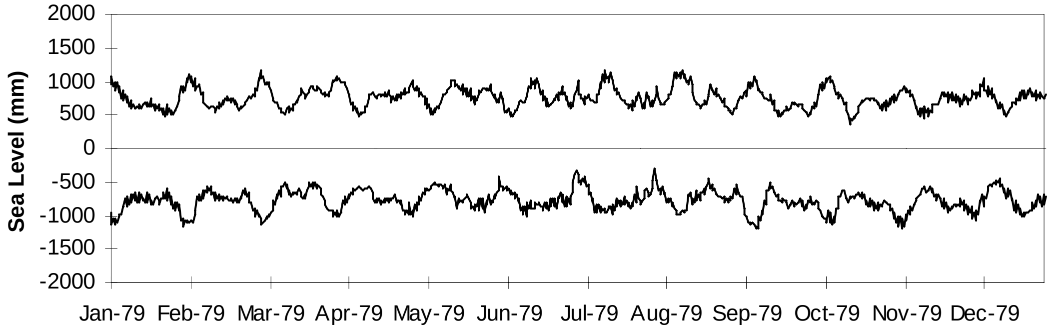
2000
1500
1000
500
0
-500
-1000
-1500
-2000
Sea Level (mm)
Jan-79 Feb-79 Mar-79 Apr-79 May-79 Jun-79 Jul-79 Aug-79 Sep-79 Oct-79 Nov-79 Dec-79

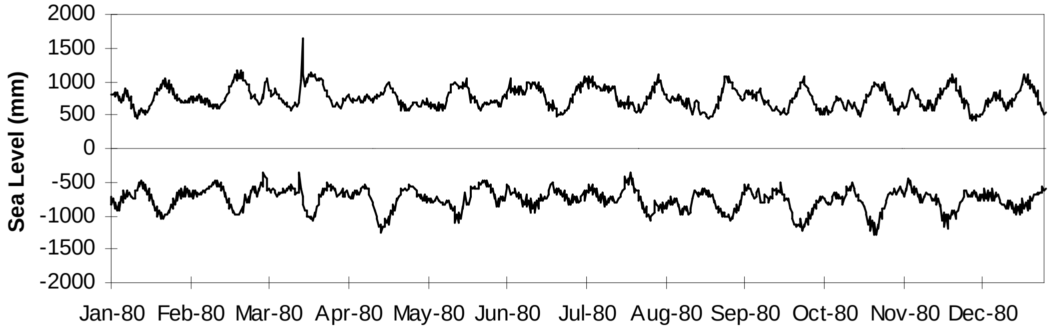
2000
1500
1000
500
0
-500
-1000
-1500
-2000
Sea Level (mm)
Jan-80 Feb-80 Mar-80 Apr-80 May-80 Jun-80 Jul-80 Aug-80 Sep-80 Oct-80 Nov-80 Dec-80

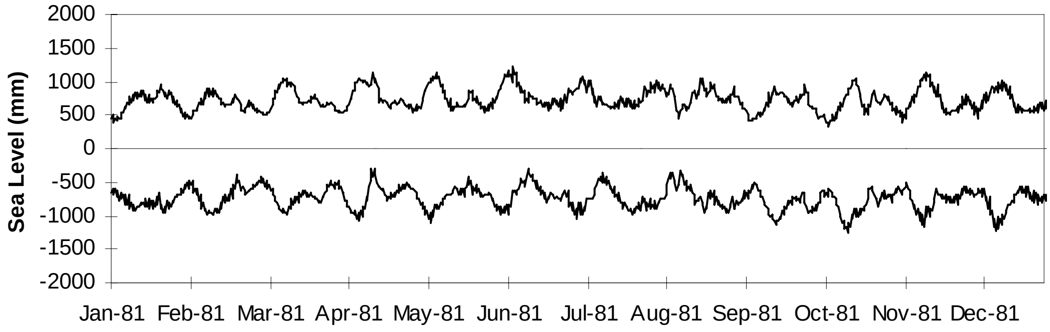
2000
1500
1000
500
0
-500
-1000
-1500
-2000
Sea Level (mm)
Jan-81 Feb-81 Mar-81 Apr-81 May-81 Jun-81 Jul-81 Aug-81 Sep-81 Oct-81 Nov-81 Dec-81

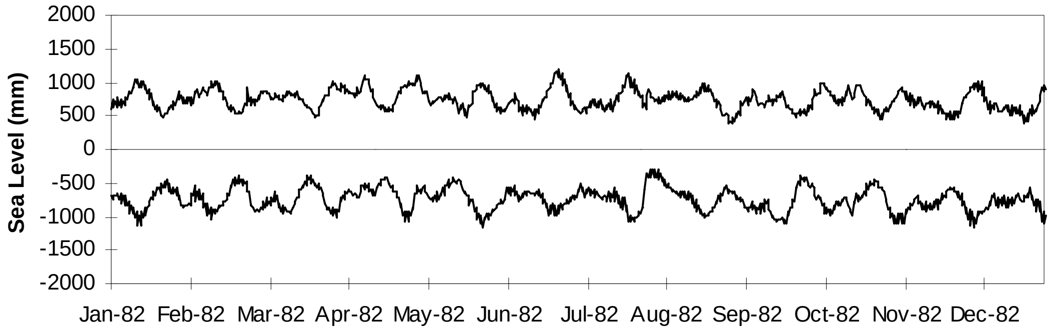
2000
1500
1000
500
0
-500
-1000
-1500
-2000
Sea Level (mm)
Jan-82 Feb-82 Mar-82 Apr-82 May-82 Jun-82 Jul-82 Aug-82 Sep-82 Oct-82 Nov-82 Dec-82

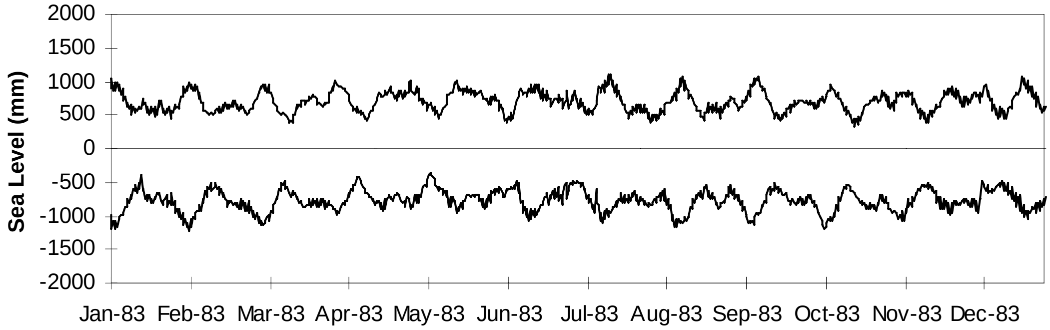
2000
1500
1000
500
0
-500
-1000
-1500
-2000
Sea Level (mm)
Jan-83 Feb-83 Mar-83 Apr-83 May-83 Jun-83 Jul-83 Aug-83 Sep-83 Oct-83 Nov-83 Dec-83

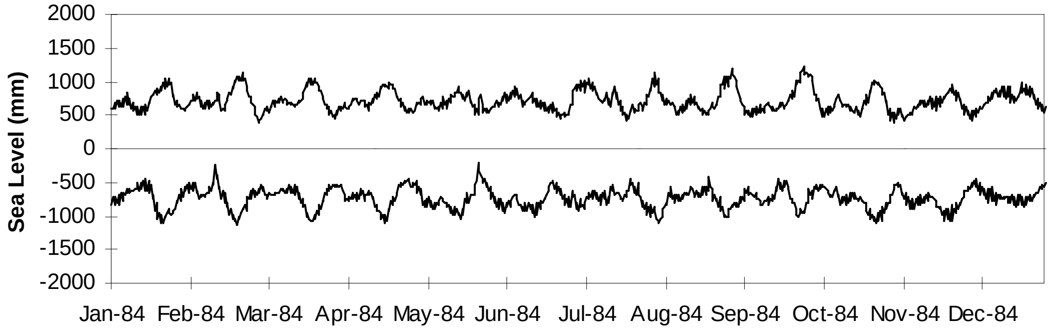
2000
1500
1000
500
0
-500
-1000
-1500
-2000
Sea Level (mm)
Jan-84 Feb-84 Mar-84 Apr-84 May-84 Jun-84 Jul-84 Aug-84 Sep-84 Oct-84 Nov-84 Dec-84

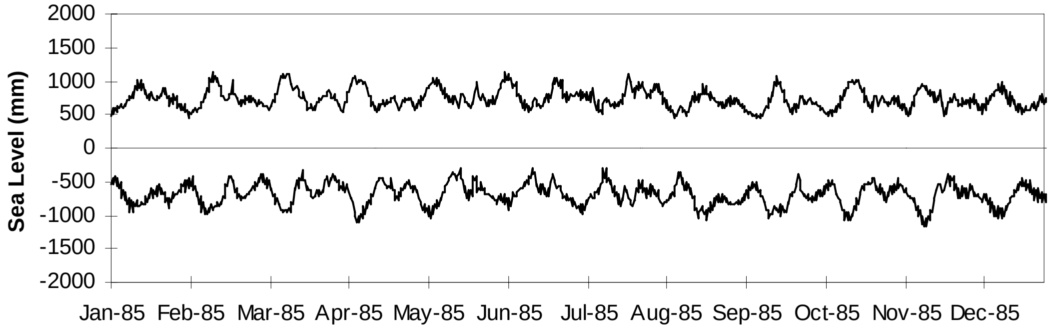
2000
1500
1000
500
0
-500
-1000
-1500
-2000
Sea Level (mm)
Jan-85 Feb-85 Mar-85 Apr-85 May-85 Jun-85 Jul-85 Aug-85 Sep-85 Oct-85 Nov-85 Dec-85

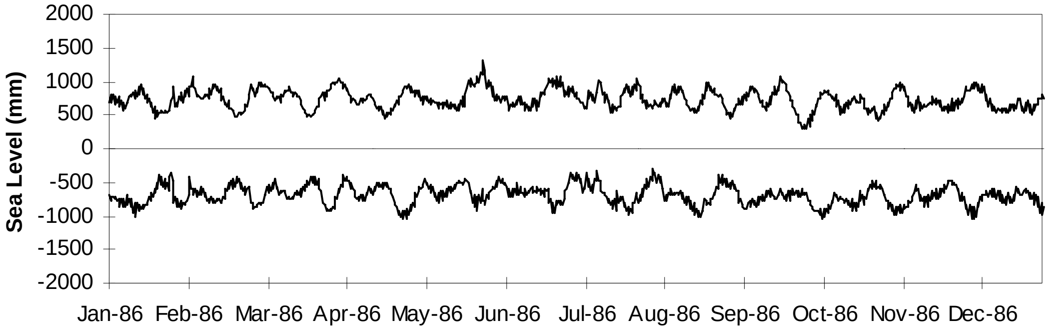
2000
1500
1000
500
0
-500
-1000
-1500
-2000
Sea Level (mm)
Jan-86 Feb-86 Mar-86 Apr-86 May-86 Jun-86 Jul-86 Aug-86 Sep-86 Oct-86 Nov-86 Dec-86

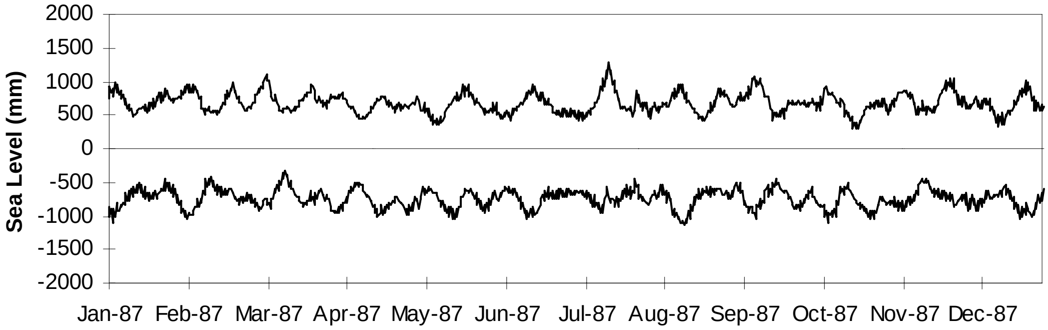
2000
1500
1000
500
0
-500
-1000
-1500
-2000
Sea Level (mm)
Jan-87 Feb-87 Mar-87 Apr-87 May-87 Jun-87 Jul-87 Aug-87 Sep-87 Oct-87 Nov-87 Dec-87

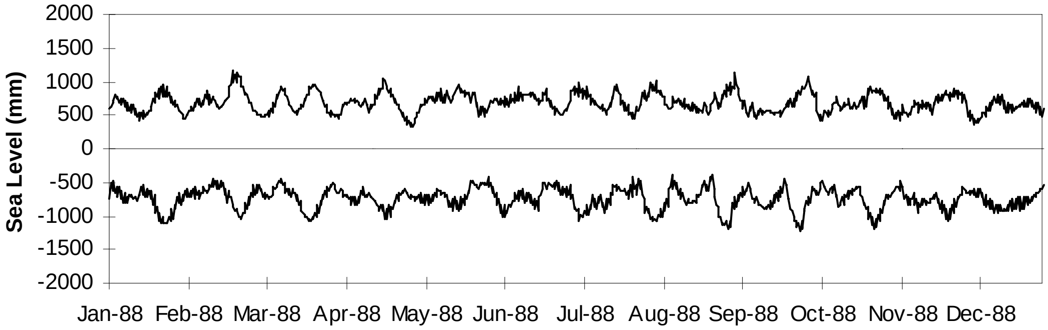
2000
1500
1000
500
0
-500
-1000
-1500
-2000
Sea Level (mm)
Jan-88 Feb-88 Mar-88 Apr-88 May-88 Jun-88 Jul-88 Aug-88 Sep-88 Oct-88 Nov-88 Dec-88

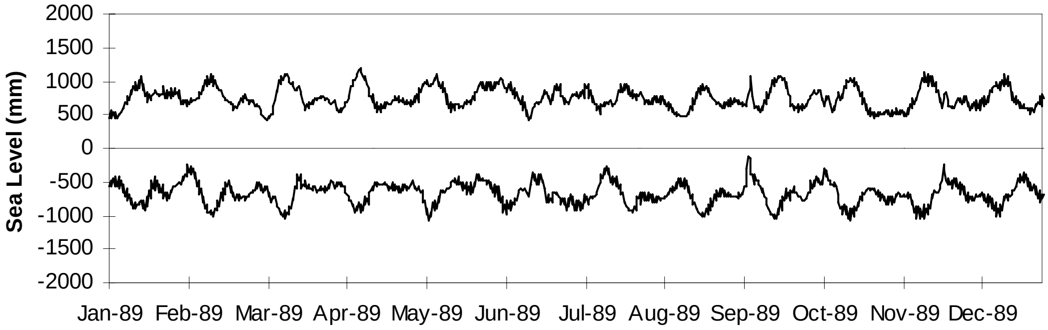
2000
1500
1000
500
0
-500
-1000
-1500
-2000
Sea Level (mm)
Jan-89 Feb-89 Mar-89 Apr-89 May-89 Jun-89 Jul-89 Aug-89 Sep-89 Oct-89 Nov-89 Dec-89

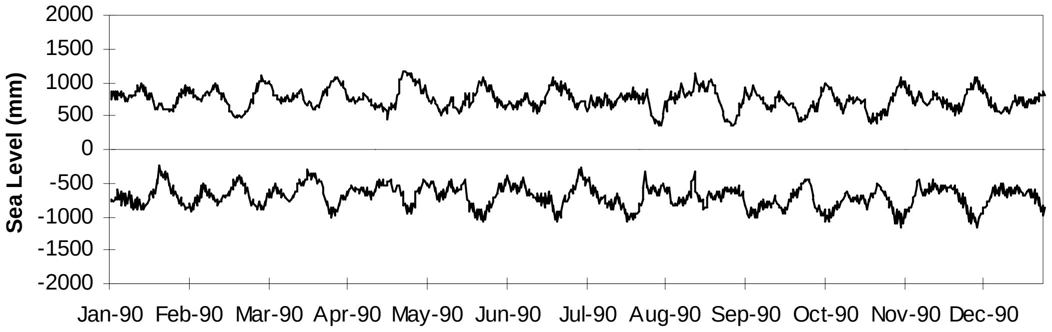
Sea Level (mm)
2000
1500
1000
500
0
-500
-1000
-1500
-2000
Jan-90 Feb-90 Mar-90 Apr-90 May-90 Jun-90 Jul-90 Aug-90 Sep-90 Oct-90 Nov-90 Dec-90

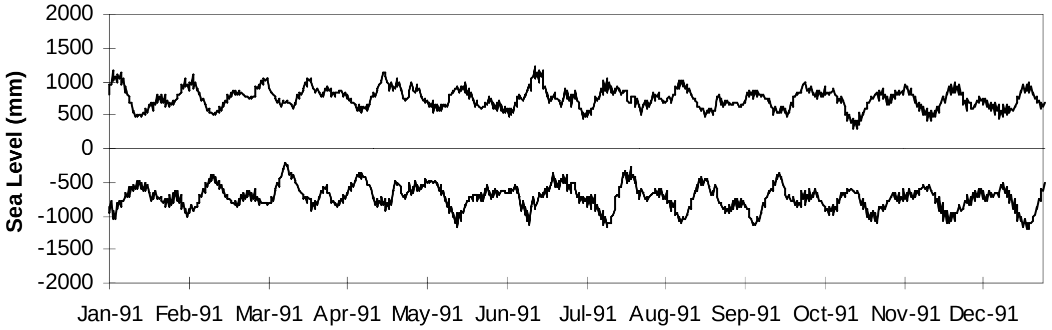
Sea Level (mm)
2000
1500
1000
500
0
-500
-1000
-1500
-2000
Jan-91 Feb-91 Mar-91 Apr-91 May-91 Jun-91 Jul-91 Aug-91 Sep-91 Oct-91 Nov-91 Dec-91

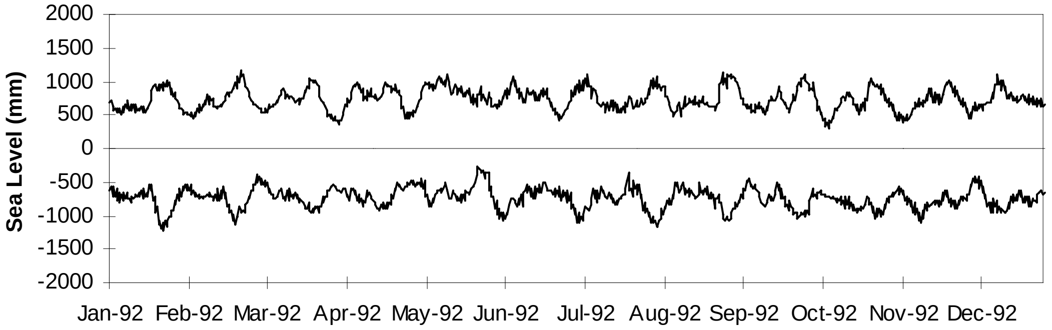
Sea Level (mm)
2000
1500
1000
500
0
-500
-1000
-1500
-2000
Jan-92 Feb-92 Mar-92 Apr-92 May-92 Jun-92 Jul-92 Aug-92 Sep-92 Oct-92 Nov-92 Dec-92

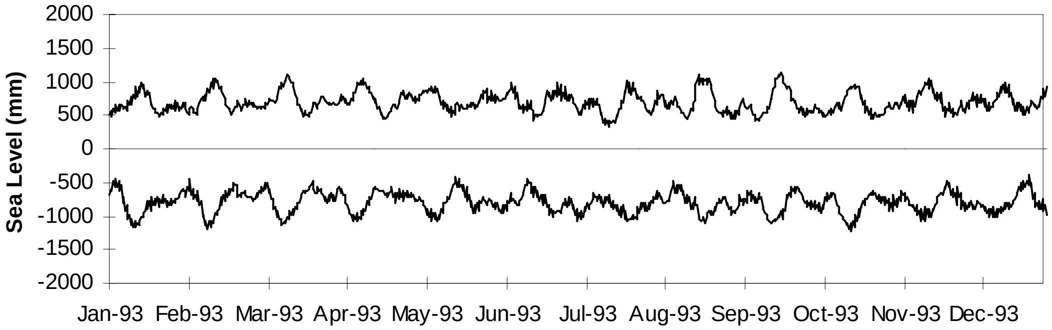
Sea Level (mm)
2000
1500
1000
500
0
-500
-1000
-1500
-2000
Jan-93 Feb-93 Mar-93 Apr-93 May-93 Jun-93 Jul-93 Aug-93 Sep-93 Oct-93 Nov-93 Dec-93

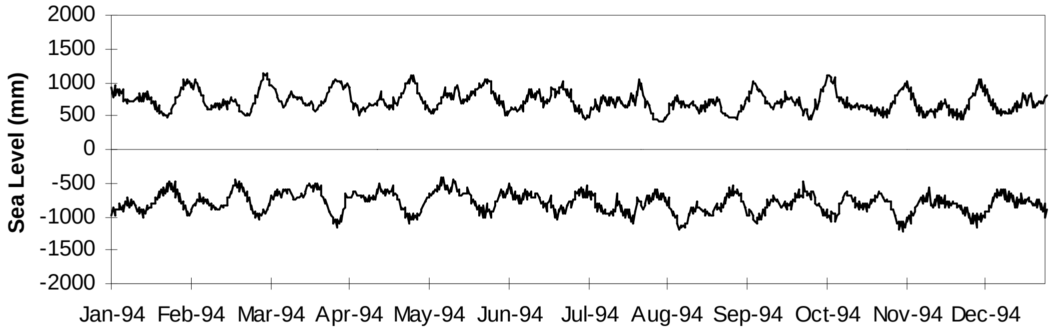
Sea Level (mm)
2000
1500
1000
500
0
-500
-1000
-1500
-2000
Jan-94 Feb-94 Mar-94 Apr-94 May-94 Jun-94 Jul-94 Aug-94 Sep-94 Oct-94 Nov-94 Dec-94

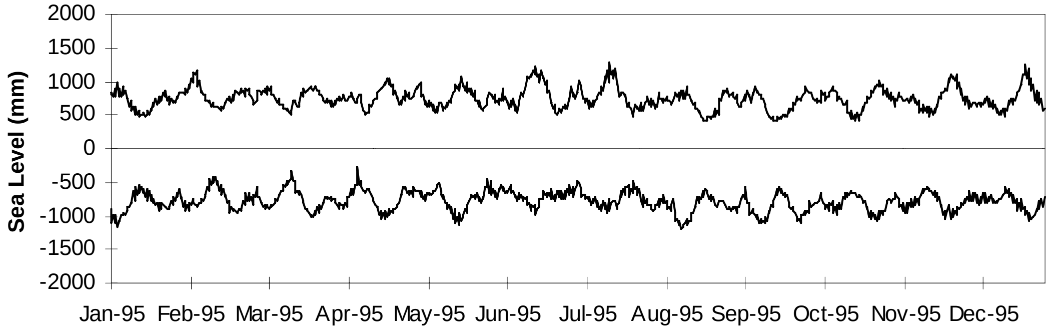
Sea Level (mm)
2000
1500
1000
500
0
-500
-1000
-1500
-2000
Jan-95 Feb-95 Mar-95 Apr-95 May-95 Jun-95 Jul-95 Aug-95 Sep-95 Oct-95 Nov-95 Dec-95

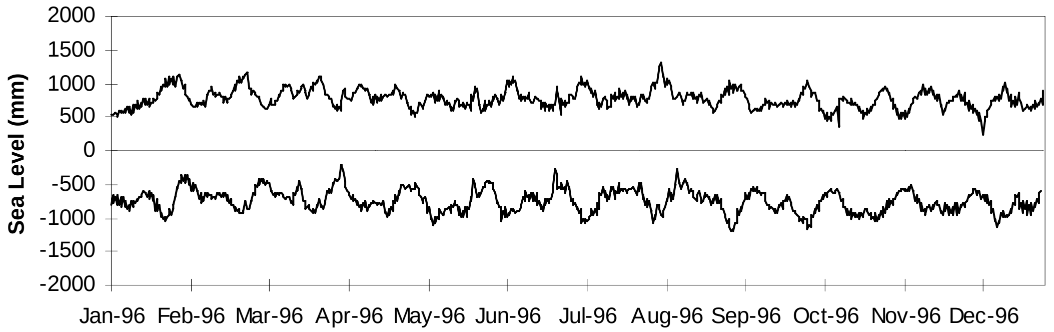
Sea Level (mm)
2000
1500
1000
500
0
-500
-1000
-1500
-2000
Jan-96 Feb-96 Mar-96 Apr-96 May-96 Jun-96 Jul-96 Aug-96 Sep-96 Oct-96 Nov-96 Dec-96